RSC Advances

PAPER

View Article Online
View Journal | View Issue

Cite this: *RSC Adv.*, 2025, **15**, 44410

Acid-enhanced ternary DES pretreatment of wheat straw guided by Kamlet–Taft parameters: boosting lignin separation and enzymatic hydrolysis

Jing-yuan Su, Yan-xia An, * Lin-lin Li, Jia-zi Wang, Yi Han, Jian Zhang and Yang Zhao

In this study, ternary deep eutectic solvent (DES) systems were constructed by introducing solid acids ($AlCl_3$, PTA, $FeBr_3$) into binary DES systems to achieve improved lignocellulose separation efficiency and enhanced enzymatic hydrolysis. Correlation analysis between the Kamlet–Taft solvatochromic parameters and lignin extraction rate/enzymatic hydrolysis efficiency revealed that the pretreatment and enzymatic hydrolysis steps were significantly improved by enhancing the hydrogen bond acidity. Accordingly, ternary DES systems with better pretreatment efficacy were screened. Notably, using the ChCl/BDO/$AlCl_3$ (25 : 50 : 1) system at 120 °C for 60 min provided the most optimal pretreatment and enzymatic hydrolysis performance for wheat straw. After pretreatment under these conditions, an 85.74% lignin extraction rate was achieved, and 72 h of enzymatic hydrolysis provided a 99.67% polysaccharide degradation rate and 74.59% reducing sugar yield. This DES system maintained good pretreatment performance even after four reuse cycles. Moreover, this pretreatment strategy demonstrated good applicability to multiple biomass types, providing a novel approach for developing efficient and environmentally friendly lignocellulose separation technologies.

Received 12th August 2025
Accepted 3rd November 2025

DOI: 10.1039/d5ra05909g

rsc.li/rsc-advances

1 Introduction

Given the unsustainability of non-renewable resources and persistent ecological degradation, lignocellulosic biomass is being increasingly recognized as a promising green, renewable, and sustainable resource.[1] Lignocellulosic biomass is typically composed of polysaccharides (cellulose and hemicellulose) and lignin, which is an aromatic polymer.[2] However, the dense structure, complex composition, cellulose crystalline regions, and lignin hydrophobic groups in lignocellulosic biomass promote the formation of stable covalent bonds and hydrogen-bond networks between biopolymers. Consequently, the structure of lignocellulosic biomass is resistant to disruption, hindering its efficient utilization.[2] To enhance the utilization efficiency of lignocellulosic biomass, a pretreatment step is required to alter the native structure and separate the target components.[3]

Deep eutectic solvents (DESs) are an emerging class of green solvents that combine the advantages of ionic liquids and organic solvents. DES systems are widely applied for the clean and efficient separation of lignocellulosic components due to their simple synthesis, low cost, strong stability, good biocompatibility, and recyclability.[4] When utilized as pretreatment agents, DES systems form strong hydrogen bonds with the components of lignocellulosic biomass, competitively disrupting the original hydrogen bond network to effectively separate the individual components.[5] DESs are formed by mixing specific stoichiometric ratios of hydrogen bond acceptors (HBA) and hydrogen bond donors (HBD) (*e.g.*, amides, carboxylic acids, polyols).[6] Choline chloride (ChCl) is widely utilized as an HBA for lignin separation due to its economic viability and biocompatibility.[6] For instance, Alvarez *et al.*[7] reported that using a lactic acid/choline chloride DES to treat poplar at 145 °C for 6 h resulted in a lignin yield of 78.5%. Tan *et al.*[8] compared the lignin separation efficiencies achieved by using different DESs to treat oil palm empty fruit bunches at 120 °C for 8 h. They showed that the lignin separation performance of acidic DESs was significantly better than that of neutral and alkaline DESs. Among them, acidic choline chloride/lactic acid exhibited optimal component separation performance, with a 100% hemicellulose extraction rate, 88% lignin removal rate, and 50% lignin extraction rate. These findings provide critical solvent selection criteria for efficient lignin separation. In a study on multicomponent DESs, Jiang *et al.* reported that introducing an acidic third component into binary DES systems markedly enhanced their lignocellulose separation efficiency.[9] The improved performance of ternary DES systems is partly because the high viscosity of DESs adversely affects biomass delignification.[3] Introducing a third component can reduce the viscosity of DESs while enhancing their solubility and stability.[10] Moreover, the addition of a third

College of Food Science and Technology, Henan Agricultural University, Zhengzhou 450002, Henan, China. E-mail: yanxiaan@henau.edu.cn

component also provides active protons and additional acidic sites as well as additional functionality.[11] The incorporation of metal chlorides enables the selective catalytic degradation of hemicellulose. Adding such metal cations to DES systems increases the number of acidic active sites, leading to improved biomass component separation.[12,13]

The solventization efficacy of DESs can be ascertained through the Kamlet–Taft solventization colorimetric parameters, a system comprising three distinct characteristic parameters: α (hydrogen bond acidity), β (hydrogen bond basicity), and π^* (polarity or polarizability).[14] In recent studies, these parameters have been employed to evaluate the pretreatment and dissolution capabilities of DESs for lignocellulose. For instance, Oh *et al.*[15] synthesized various choline chloride-based DESs for pine wood pretreatment, finding that the efficiency of biomass pretreatment using DESs increased with their polarity (π^*) and hydrogen bonding acidity (α). Furthermore, a positive linear correlation was observed between α and lignin extraction efficiency. Zhang *et al.*[16] prepared a series of DESs with different HBAs and HBDs to dissolve lignocellulosic components, revealing that DESs with higher α–β (net acidity) values were more effective in dissolving cellulose. It was also noted that the solubility of xylan increased with the β value of the DES. Sanders *et al.*[17] determined the Kamlet–Taft parameters of DESs composed of choline chloride and five carboxylic acids, using hardwood and softwood raw materials for DES pretreatment experiments. They found a positive correlation between the lignin removal rate and both the α value and net acidity value of the DES.

DES solvent systems demonstrate favorable extraction performance in lignin separation applications, achieving lignin dissolution rates that generally exceed 50%. However, the industrial implementation of these systems still faces challenges. For instance, existing processes commonly require high operating temperatures and prolonged reaction times, leading to significantly higher production costs and impeding the development of continuous production processes.[14] Therefore, developing more efficient and milder methods to enhance DES-based lignin separation will be crucial for industrial applications. Although several studies have reported the solvatochromic parameters of some DESs, the available data remains insufficient when compared to the existing system and the potential for new DESs.[16] Notably, there is a significant gap in understanding the relationship between the lignin extraction rate, enzymatic hydrolysis efficiency, and Kamlet–Taft related parameters of DESs. Building upon binary DES systems for wheat straw lignin separation, this study constructed ternary DES systems by introducing solid acids as catalysts. These ternary DESs were used to pretreat the wheat straw with the goal of achieving an improved lignin extraction rate and enzymatic hydrolysis efficiency. The ternary DES systems that demonstrated solvatochromic parameters performance were screened by measuring their solvatochromic parameters for DES performance optimization. Subsequently, the reaction parameters were optimized. These identified optimal conditions were then applied to other types of biomass, thereby providing a reference for the selective design of solvent systems and facilitating green and efficient lignin separation.

2 Materials and methods

2.1. Materials

Wheat straw, rice straw, corncob, and corn straw were sourced from the Wheat Experimental Base of Henan Agricultural University. Eucalyptus wood was provided by the College of Forestry, Henan Agricultural University. All natural materials were sun-dried, pulverized, dewaxed, sieved through a 60-mesh sieve, dried, and stored in desiccators for later use. Choline chloride (ChCl), 1,4-butanediol (BDO), ethylene glycol (EG), glycerol (GL), aluminium chloride ($AlCl_3$) and ferric bromide ($FeBr_3$) were purchased from Shanghai Macklin Biochemical Technology Co., Ltd. PTA was obtained from Tianjin Damao Chemical Reagent Factory. Other reagents were of analytical grade.

2.2. Preparation of DESs

The reagents should be accurately mixed according to their respective molar ratios: ChCl/BDO (1 : 2), ChCl/EG (1 : 2), ChCl/GL (1 : 2, 1 : 4), ChCl/BDO/$AlCl_3$ (25 : 25 : 0.5, 25 : 50 : 0.5, 25 : 50 : 1), ChCl/EG/PTA (25 : 25 : 0.025, 25 : 50 : 0.025, 25 : 50 : 0.05), and ChCl/GL/$FeBr_3$ (25 : 50 : 0.25, 25 : 100 : 0.25, 25 : 100 : 0.5). Each mixture was stirred at 70 °C until a homogeneous transparent liquid was formed to obtain the corresponding DES. The resulting DESs were placed in desiccators for further use.

2.3. Determination of Kamlet–Taft solvatochromic parameters of DESs

Nile red, 4-nitroaniline (NH_2), and *N*,*N*-diethyl-4-nitroaniline (NEt_2) were dissolved in anhydrous methanol to prepare 0.05 mM dye solutions, which were protected from light before their further use.[9] 5 mL aliquots of the dye solutions were transferred to 10 mL centrifuge tubes, and the tubes were vacuum-dried to remove the methanol. Then, 3 mL of a different DES was added to each tube and thoroughly mixed with the dyes. Detection was performed using a UV-vis spectrophotometer within the scanning wavelength range of 300–700 nm. The following equations were used to calculate the Kamlet–Taft solvatochromic parameters α, β, and π^* of the different DESs:[18]

$$\pi^* = 0.314 \times (27.52 - \nu(NEt_2)) \quad (1)$$

$$\alpha = \frac{19.9657 - 1.0241 \times \pi^* - \nu(NR)}{1.6078} \quad (2)$$

$$\beta = \frac{11.134 - 3580}{\lambda_{max}(NH_2)} - 1.125 \times \pi^* \quad (3)$$

Here: α is the hydrogen bonding acidity; β is the hydrogen bonding basicity; π^* is the polarizability; λ_{max} is the maximum absorption wavelength of each dye; ν is the staining wavenumber of each dye, $\nu = 1/(\lambda_{max} \times 10^{-4})$.

2.4. Pretreatment of wheat straw with DESs

Wheat straw was uniformly mixed with a DES using a solid-to-liquid ratio of 1 : 20. Each mixture was heated under stirring at a specified temperature (100 °C, 110 °C, 120 °C, 130 °C, 140 °C) for a defined duration (20 min, 30 min, 40 min, 60 min, 80 min, 100 min). An anhydrous ethanol–water solution (7 : 3 v/v) was added to the pretreated mixtures, which were then magnetically stirred for 30 min. Solid–liquid separation was achieved through repeated centrifugation and washing. The supernatant from each mixture was rotary-evaporated to remove the ethanol, yielding a lignin-DES solution. Deionized water was then added to this lignin-DES solution, and the combined solution was stored at 4 °C for static precipitation. Finally, lignin was separated by centrifuging the mixture, and freeze-drying was employed to obtain an absolute dry lignin sample.

2.5. Composition analysis

The polysaccharide and lignin contents of the untreated and pretreated wheat straw were determined according to NREL analytical procedures.[19] Specifically, 30 mg samples of wheat straw or pretreated residues were hydrolyzed with 0.3 mL of 72% sulfuric acid at 30 °C for 1 h. Each mixture was then diluted to 4% acid concentration by adding 8.4 mL of distilled water, and hydrolysis was performed at 121 °C (0.1 MPa) for 1 h. After the reaction, the hydrolysates were filtered through pre-dried (105 °C to constant weight) G4 glass sintered funnels under a vacuum. The filtrates were then divided: one portion was neutralized with calcium carbonate to determine the reducing sugar concentration *via* the 3,5-dinitrosalicylic acid (DNS) method, enabling the polysaccharide content to be calculated. The other portion was analyzed *via* UV spectrophotometry at 320 nm, and the acid-soluble lignin (ASL) content was calculated using an extinction coefficient of 30 L g^{-1} cm^{-1}. The residual solids adhered to the tube were rinsed into funnels with distilled water and repeatedly washed to prevent the carbonization of the carbohydrates during drying. The residues were then oven-dried at 105 °C for at least 4 h to constant weight and weighed. Subsequently, the residues were ashed in a muffle furnace at 575 °C for 3 h to a constant weight to quantify the acid-insoluble lignin (AIL) content. The lignin extraction rate and residue recovery rate were calculated using the following formulas:

$$\text{Lignin extraction rate}(\%) = \left(1 - \frac{\text{Lignin amount in the recovered residue}}{\text{Lignin amount in the native biomass}}\right) \times 100 \quad (4)$$

$$\text{Residue recovery rate}(\%) = \frac{\text{Recycled residue amount}}{\text{Native biomass amount}} \times 100 \quad (5)$$

2.6. Enzymatic hydrolysis analysis

20 mg of untreated or pretreated wheat straw, 20 FPU per g substrate cellulase, 7 mL preheated (50 °C) citrate buffer (50 mM, pH 4.8), and 20 μg mL^{-1} sodium azide were weighed and added to a 25 mL ground-glass stoppered conical flask. The timed reaction was performed in a constant-temperature incubator shaker at 50 °C with 200 rpm agitation. At regular intervals, 0.3 mL aliquots were removed and inactivated in a boiling water bath for 5 min to terminate the enzymatic reactions. Centrifugation (10 000 rpm, 5 min) was then performed using a high-speed refrigerated centrifuge, and the DNS method was used to determine the reducing sugar concentration. The polysaccharide degradation rate and reducing sugar yield were calculated using the following formulas:

$$\text{Polysaccharide degradation rate}(\%) = \frac{\text{Released reducing sugar amount in enzymatic} \times 0.9}{\text{Polyaccharide amount in the enzymatic sample}} \times 100 \quad (6)$$

$$\text{Reducing sugar yield}(\%) = \frac{\text{Released reducing sugar amount}}{\text{Theoretic reducing sugar amount in the untreated samples}} \times 100 \quad (7)$$

Here: 0.9 is the factor used to convert the reducing sugar content to the equivalent polysaccharide content.

2.7. Determination of reducing sugar concentration by the DNS method

The reducing sugars were quantified according to the IUPAC DNS methodology.[20] First, 0.2 mL of centrifuged enzymatic hydrolysate was diluted to 2 mL with distilled water. Next, 3 mL of DNS reagent was added, and a reaction was performed in a boiling water bath for 5 min. The reacted mixture was cooled to room temperature using cold water and then appropriately diluted with distilled water. Finally, the absorbance was measured at 540 nm using a spectrophotometer.

2.8. Recycling of DES

Following the DES pretreatment of wheat straw, both the washing solution and the filtrate derived from the solid residue are collected and amalgamated. Subsequently, a vacuum rotary evaporator is employed to eliminate moisture at a temperature of 70 °C until a consistent weight is attained. The recovered DES is then repurposed for subsequent pretreatment reactions. This DES recovery procedure is iteratively carried out using the method described above.

$$\text{DES recovery rate}(\%) = \frac{\text{Quality of DES recovery}}{\text{Quality of DES used}} \times 100 \quad (8)$$

2.9. Characterization of natural materials and solid residues

Fourier transform infrared spectroscopy (FTIR, Nicolet iS50, Thermo, USA) was utilized to characterize the natural biomass materials and solid residues pretreated with the DESs. Each sample was thoroughly ground, mixed with potassium bromide (KBr) powder, and then pressed into a transparent pellet. Full-range scanning (400–4000 cm^{-1}) was performed using an FTIR

spectrometer at a resolution of 0.4 cm^{-1}. Structures were analyzed in transmittance mode.

X-ray diffraction (XRD, ULTIMA IV, Rigaku, Japan) was utilized to evaluate the crystal structures of the biomass samples before and after pretreatment. Diffraction patterns were obtained in the 2θ range of 5–60° using a speed of 5° min^{-1}, step size of 4°, voltage of 40 kV, and current of 40 mA. The crystallinity index (CrI) was calculated using the following formula:

$$\mathrm{CrI}(\%) = \frac{I_{002} - I_{\mathrm{am}}}{I_{002}} \times 100 \quad (9)$$

Here: I_{002} is the diffraction intensity of the 002 crystal plane ($2\theta \approx 22°$) and I_{am} is the diffraction intensity in the amorphous region ($2\theta \approx 18°$).

Scanning electron microscopy (SEM, Gemini 300, Zeiss, Germany) was used to analyze the surface morphology of the pretreated materials. Before testing, the sample powders were uniformly dispersed on metal stubs with a conductive adhesive and then sputter-coated with gold.

2.10. Characterization of lignin

Prior to conducting analysis *via* gel permeation chromatography (GPC, PL-GPC50, Agilent, USA), lignin samples necessitate acetylation treatment. The acetylation pretreatment method employed in this study followed the approach outlined by Wang *et al.*[21]

The lignin samples were dissolved in DMSO-d_6 at 25 °C and detected by Bruker Biospin's AVANCE III 600 MHz fully digital superconducting nuclear magnetic resonance spectrometer. The chemical structure of lignin samples was evaluated by two-dimensional ^{13}C–^{1}H heteronuclear single quantum correlation nuclear magnetic resonance (2D-HSQC).

Semi-quantitative analysis of the relevant linkages was carried out based on the 2D NMR spectra, utilizing the following calculation formulas:[22]

$$I(\mathrm{C_9})\mathrm{units} = 0.5I(S_{2,6}) + I(G_2) \quad (10)$$

The calculation is based on the following formula:

$$I(X)\% = \frac{I(X)}{I(\mathrm{C_9})} \times 100 \quad (11)$$

Here, $I(X)$ is defined as the ratio of the integral value corresponding to the α-C-H correlation peak of structure A (β-O-4′) to the integral value of the $I(\mathrm{C_9})$ element, where A represents the integral value measured at the same contour level.

The numerical calculation formula of S/G is as follows:

$$\frac{S}{G} = 0.5I\left(S_{2/6}\right)/I(G_2) \quad (12)$$

Here, $I(\mathrm{S_{2/6}})$ signifies the combined sum of the C–H peak integrals at positions 2 and 6 of both the lilac base structure (S) and its oxidized counterpart (S'); whereas $I(G_2)$ indicates the C–H peak integral value at position 2 of the guaiacol base structure (G).

2.11. Statistical analysis

All laboratory analyses were performed in triplicate to ensure reproducibility. The figures in this work present results as the mean ± standard deviation (error bars).

3 Results and discussion

3.1. Analysis of DES solvatochromic parameters

Kamlet–Taft solvatochromic parameters are widely used to characterize the microscopic physicochemical properties of solvents. The parameters α and β respectively represent hydrogen bond acidity (proton-donating ability) and basicity (proton-accepting ability), while π* indicates solvent dipolarity/polarizability.[23] The π* value reflects the strength of cation–anion interactions. Meanwhile, higher α and β values significantly impact pretreatment efficiency: elevated α values facilitate proton dissociation, while increased β values enhance the acceptance of hydrogen bonds by anions.[24] Thus, the Kamlet–Taft solvatochromic parameters of a DES can quantify the ease of hydrogen bond formation, enabling a preliminary prediction of pretreatment efficiency. As shown in Table 1, adding solid acids ($AlCl_3$, PTA, $FeBr_3$) to the prepared DESs as third components increased their π* and α values to varying degrees. Higher α values indicate enhanced solvent acidity, which may promote ether bond cleavage in lignocellulose. DESs with high α values readily donate hydrogen bonds to release H^+, making α a critical factor for lignin extraction efficiency.[25] Solvent polarity (indicated by π*) affects activation energy and solubility.[16] The ternary DESs exhibited higher π* values than the binary systems, indicating stronger ion–ion interactions. Based on the enhancement of solvent acidity and polarity reflected by the elevated α and π values observed in Table 1, it was preliminarily predicted that the three ternary DES, ChCl/BDO/$AlCl_3$ (25 : 50 : 1), ChCl/EG/PTA (25 : 50 : 0.05), and ChCl/GL/$FeBr_3$ (25 : 100 : 0.5), had a better pretreatment for wheat straw effect.

3.2. Effects of DES composition on wheat straw pretreatment and enzymatic hydrolysis

The impact of DES composition on wheat straw pretreatment was evaluated under standardized conditions (120 °C, 1 h), as shown in Fig. 1. The diol-based binary DES systems exhibited uniformly low pretreatment and enzymatic hydrolysis efficiencies, with statistically insignificant variations. However, the incorporation of solid acids ($AlCl_3$, PTA, $FeBr_3$) to obtain ternary DES formulations significantly enhanced both efficiency metrics relative to the binary systems. The ChCl/BDO/$AlCl_3$ (25 : 50 : 1) system exhibited the best performance, achieving 85.74% lignin extraction, 99.67% polysaccharide degradation (after 72 h), and a reducing sugar yield of 74.59%. These values substantially exceeded those of the ChCl/BDO (1 : 2) benchmark (13.63%, 56.17%, 45.69%), and the residue recovery decreased to 49.92% *versus* 73.85% for the binary system. In prior studies, Wang *et al.*[21] utilized a newly developed deep eutectic solvent (DES) derived from hardwood lignin, formulated with *p*-hydroxybenzoic acid (PB) and choline chloride (ChCl). This DES was employed to effectively pretreat lignocellulosic biomass at 160 °C for a duration of 3 hours, resulting in

Table 1 Kamlet–Taft solvatochromatic parameters of prepared DESs

Composition of DES	Molar ratio of components	π*	α	β
ChCl/BDO	1/2	1.26 ± 0.05	1.24 ± 0.07	0.49 ± 0.14
ChCl/BDO/$AlCl_3$	25/25/0.5	1.42 ± 0.03	1.71 ± 0.05	0.34 ± 0.03
ChCl/BDO/$AlCl_3$	25/50/0.5	1.35 ± 0.05	2.01 ± 0.08	0.52 ± 0.14
ChCl/BDO/$AlCl_3$	25/50/1	1.53 ± 0.07	2.39 ± 0.09	0.31 ± 0.13
ChCl/EG	1/2	1.14 ± 0.04	1.20 ± 0.07	0.82 ± 0.03
ChCl/EG/PTA	25/25/0.025	1.27 ± 0.11	1.68 ± 0.05	0.62 ± 0.20
ChCl/EG/PTA	25/50/0.025	1.24 ± 0.04	1.93 ± 0.02	0.86 ± 0.12
ChCl/EG/PTA	25/50/0.05	1.39 ± 0.15	2.04 ± 0.13	0.50 ± 0.19
ChCl/GL	1/2	1.17 ± 0.04	1.15 ± 0.05	0.63 ± 0.07
ChCl/GL	1/4	1.09 ± 0.06	1.43 ± 0.08	0.94 ± 0.11
ChCl/GL/$FeBr_3$	25/50/0.25	1.28 ± 0.05	1.46 ± 0.17	0.45 ± 0.03
ChCl/GL/$FeBr_3$	25/100/0.25	1.27 ± 0.09	1.84 ± 0.07	0.53 ± 0.11
ChCl/GL/$FeBr_3$	25/100/0.5	1.44 ± 0.09	1.97 ± 0.07	0.44 ± 0.08

a lignin removal rate of 69%. Notably, this pretreatment method preserved high enzyme digestibility rates, with 90.8% for glucan and 88.9% for xylan. Meanwhile, Tian *et al.*[26] synthesized a binary DES using ChCl and malic acid (MA) for poplar pretreatment. After a 4-hour reaction at 120 °C, they achieved a lignin removal rate of 75.30%. The ChCl/BDO/$AlCl_3$ (25 : 50 : 1) system demonstrated superior lignin extraction rates and enzymatic digestion efficiency compared to previously reported binary DES pretreatments, while also offering the benefits of milder reaction conditions and shorter processing times. Notably, the lignin extraction efficiency demonstrated composition-dependent variation. Both alcoholic and acidic components enhanced delignification, while acidic constituents promoted lignin separation. This was because the acidic components provided supplementary protons, facilitating the cleavage of lignocellulosic bonds (ether/ester linkages, polysaccharides).[24,27] The deposition of lignin on cellulose surfaces has been reported to critically constrain enzymatic hydrolysis through dual mechanisms.[28] This deposition creates a physical barrier that limits enzyme accessibility, and the irreversible adsorption of cellulase *via* hydrophobic interactions reduces the effective enzyme concentration.[29] In this work, ternary DES pretreatment induced progressive xylan/lignin removal at elevated temperatures, resulting in complete cellulose exposure. This structural modification increased the accessibility of cellulose binding sites while reducing non-productive enzyme adsorption, leading to an enhancement in the enzymatic hydrolysis efficiency.

3.3. Correlation assessment of solvatochromic parameters with lignin extraction rate and enzymatic hydrolysis efficiency

Positive correlations were observed between the lignin extraction rates from the DES-pretreated samples and the Kamlet–Taft parameters α and α–β, as displayed in Fig. 2(a and b). Changing the DES composition affected the lignin extraction efficiency. Solid acid incorporation substantially enhanced delignification, which was attributed to the strong hydrogen bonding between the solid acids and ChCl facilitating the cleavage of lignocellulosic linkages and increasing lignin

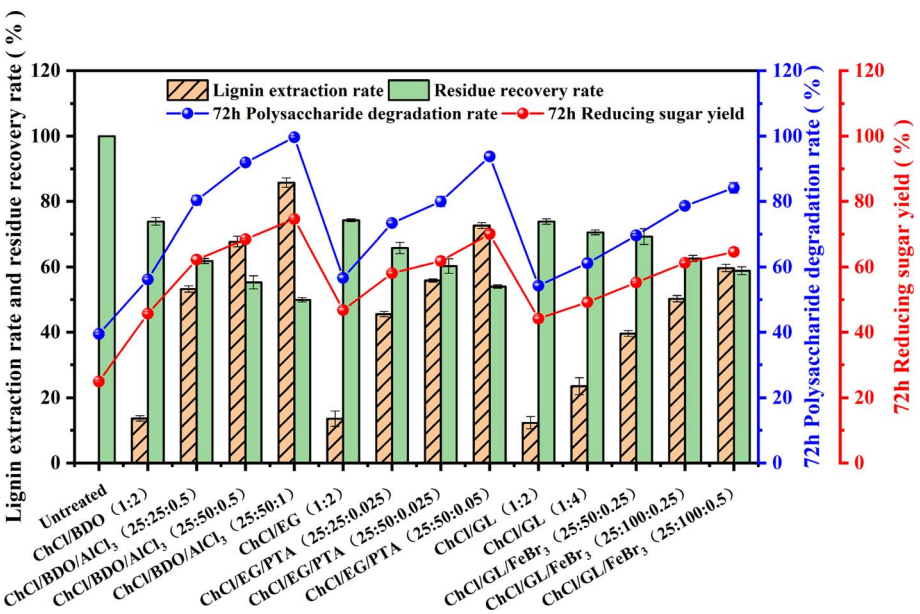

Fig. 1 Effects of different DES types and molar ratios on pretreatment and enzymatic hydrolysis of wheat straw.

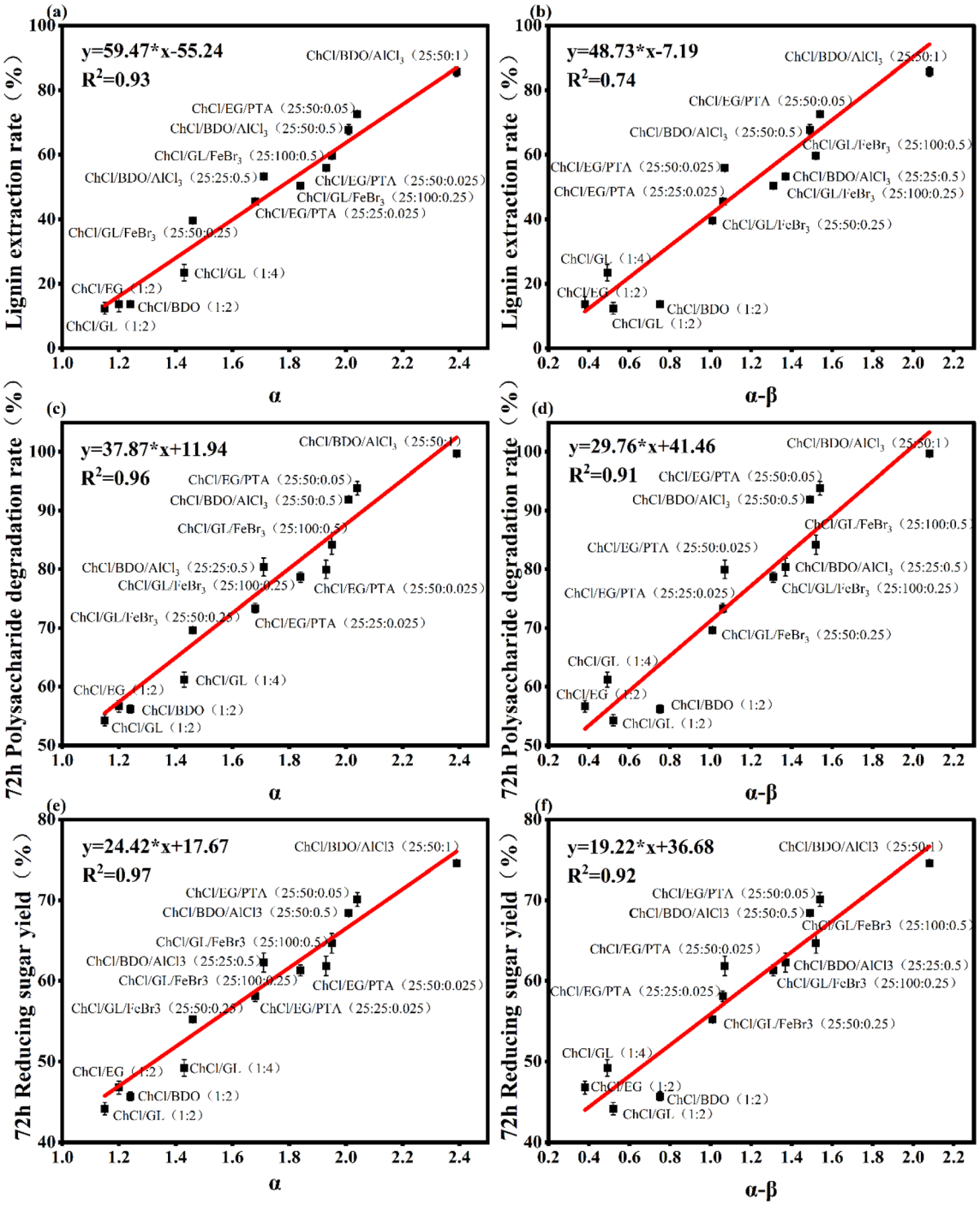

Fig. 2 Correlations between lignin extraction rate (a and b), polysaccharide degradation rate (c and d), reducing sugar yield (e and f), and Kamlet–Taft solvatochromatic parameters (α and α–β) of different DES pretreatment systems.

dissolution.[30] Positive correlations were also observed between the polysaccharide degradation rates and reducing sugar yields (72 h enzymatic hydrolysis) with parameters α and α–β, as shown in Fig. 2(c and f). The introduction of solid acids significantly improved the saccharification metrics, which was likely due to hydrogen bond-mediated cleavage in the lignocellulose.[31] When cellulose undergoes enzymatic hydrolysis, residual lignin impedes the hydrolysis process by restricting the accessibility of the enzymes to carbohydrates. After pretreatment by solid acid-catalyzed DES, wheat straw removes the vast majority of lignin, and the contact area of cellulase enzyme with the bare cellulose increases, thus improving the enzymatic efficiency.[32] DES with a higher α-value has better hydrogen bond supplying ability and can catalyze the breaking of the ether bond, glycosidic bond and LCC linkage, thus more favorable for the separation and extraction of lignin, and DES with higher hydrogen bonding acidity (α-value) is more efficient in the separation of lignin.[18,33] Higher α values were correlated

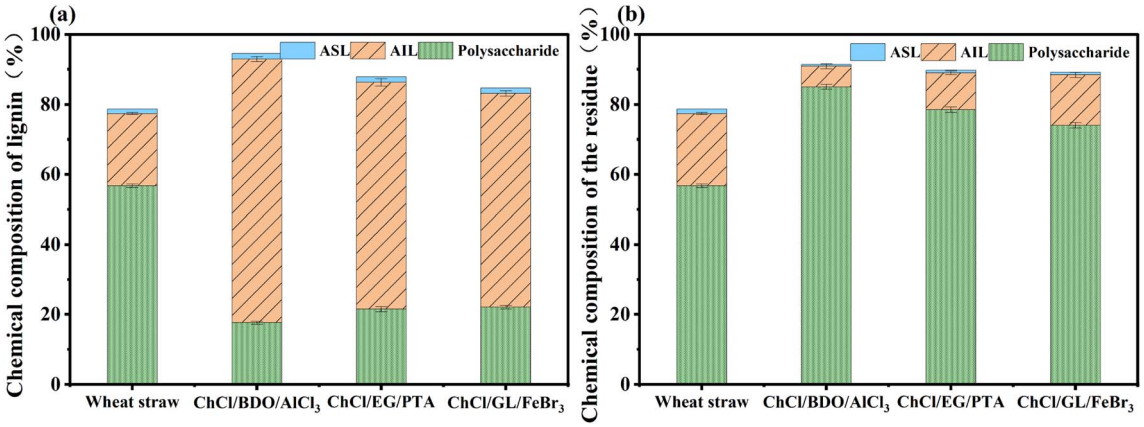

Fig. 3 Chemical composition distribution (acid-insoluble lignin (ASL) content, acid-soluble lignin (AIL) content, and polysaccharide content) of lignin (a) and solid residue (b) samples obtained using different DES pretreatment systems.

with greater lignin removal during pretreatment, reducing the residual lignin content in solids and improving enzymatic digestibility. The parameter α–β serves as an indicator of the net acidity of DESs. The lignin extraction rate and enzymatic digestibility efficiency of samples subjected to pretreatment with various DESs exhibited a positive correlation with the α–β values. This phenomenon could potentially be ascribed to the elevated net acidity observed in acidic DESs, which endow them with a higher net capacity for hydrogen donation. Consequently, this enhanced hydrogen-donating ability facilitates the dissolution of lignin.[16] Based on these relationships, three optimal ternary DES systems were identified for subsequent experimentation: ChCl/BDO/$AlCl_3$ (25 : 50 : 1), ChCl/EG/PTA (25 : 50 : 0.05), and ChCl/GL/$FeBr_3$ (25 : 100 : 0.5).

3.4. Compositional analysis of lignin and solid residues

The compositional analysis of the lignin and solid residues derived from the evaluated ternary DES pretreatment systems is presented in Fig. 3. As shown in Fig. 3(a), the ChCl/BDO/$AlCl_3$-extracted wheat straw lignin exhibited the highest purity (>75%). This lignin had an acid-soluble lignin (ASL) content of 75.33% and an acid-insoluble lignin (AIL) content of 1.62%, with both values significantly exceeding those of natural wheat straw lignin. As shown in Fig. 3(b), the DES-pretreated residues exhibited substantially reduced lignin content and enhanced polysaccharide levels (74.11–85.10%) compared to the untreated biomass (baseline: 56.77%). The enrichment of polysaccharides was ascribed to the progressive xylan/lignin removal that occurred during DES pretreatment, which facilitated the complete exposure of the cellulose. This structural modification has been reported to increase the accessibility of cellulose binding sites while reducing non-productive cellulase adsorption *via* lignin reduction, leading to enhanced enzymatic hydrolysis yields.[34] These findings confirm that ternary DES pretreatment effectively fractionates the lignocellulosic components, achieving efficient delignification and improved enzymatic saccharification.

3.5. Effects of reaction temperature and duration on wheat straw pretreatment

Mix wheat straw with ChCl/BDO/$AlCl_3$ (25 : 50 : 1) and mix thoroughly. Pretreat the mixture at different temperatures for a certain period of time to investigate the effects of reaction temperature and time on the pretreatment of wheat straw and optimize the reaction conditions. As shown in Fig. 3, with increasing reaction

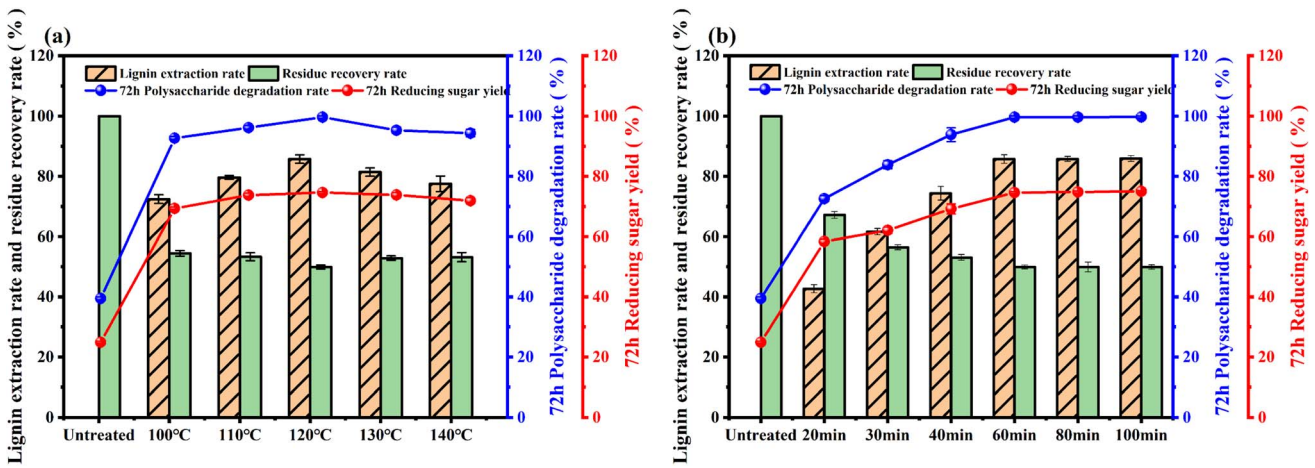

Fig. 4 Effects of reaction temperature (a) and time (b) on pretreatment and enzymatic hydrolysis.

temperature, both the lignin extraction rate and enzymatic hydrolysis efficiency exhibit a trend of first increasing and then decreasing, with the overall order being 120 °C > 110 °C > 130 °C > 140 °C. The residue recovery rate, however, shows the opposite trend. Higher temperatures tend to cause the dissociation of lignin components. However, when the pretreatment temperature rises to the decomposition onset temperature of a certain component in the DES, the strength of hydrogen bonding in the system gradually weakens, leading to a reduction in the DES's ability to decompose lignin.[35] Therefore, optimizing the pretreatment temperature can improve lignin extraction efficiency.[36] At the same reaction temperature (120 °C), as the pretreatment time increased, the lignin extraction rate, polysaccharide degradation rate, and reducing sugar yield all significantly increased, from 42.64%, 72.60%, and 58.41% at 20 min to 85.74%, 99.67%, and 74.59% at 60 min, after which they tended to plateau. This indicates that pretreatment time significantly affects lignin extraction efficiency. As pretreatment time increases, the extent of lignin removal increases, resulting in lower lignin content in cellulose, which facilitates enzymatic hydrolysis. When reaction time was extended to 80 min and 100 min, lignin extraction rate and enzymatic hydrolysis efficiency only slightly increased and remained nearly constant. Therefore, selecting a pretreatment time of 60 min is more economically efficient. The above results indicate that a reaction temperature of 120 °C and a reaction time of 60 minutes are appropriate. Under these conditions, DES demonstrates excellent lignin separation and extraction capabilities as well as enzymatic hydrolysis efficiency (Fig. 4).

3.6. Pretreatment of diverse biomasses with ChCl/BDO/$AlCl_3$ under optimal conditions

The optimal pretreatment conditions were identified as treatment with ChCl/BDO/$AlCl_3$ (25 : 50 : 1) at 120 °C for 60 min. Under these parameters, five biomass types (wheat straw, rice straw, corncob, corn straw, eucalyptus wood) were treated with

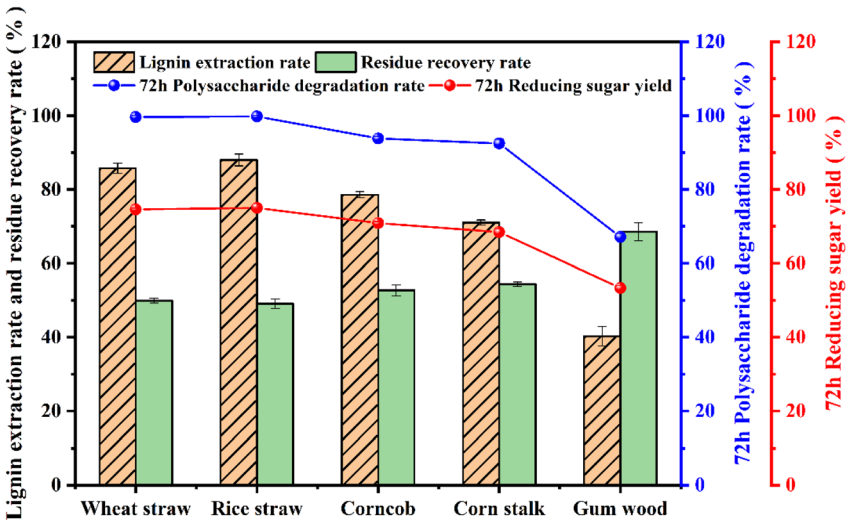

Fig. 5 Effects of ChCl/BDO/$AlCl_3$ on pretreatment and enzymatic hydrolysis of different biomasses.

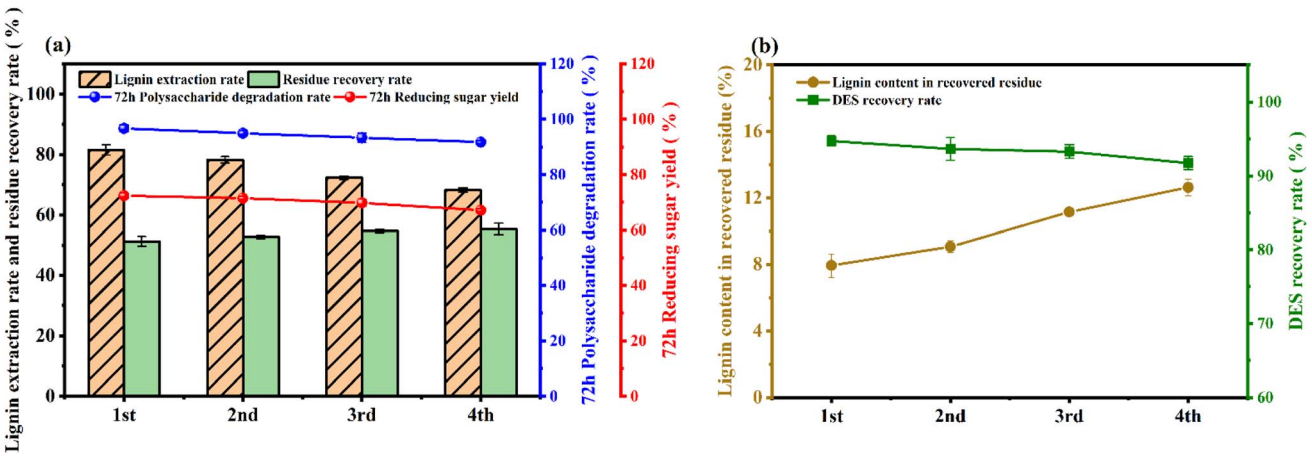

Fig. 6 The effect of recycling ChCl/BDO/$AlCl_3$ on wheat straw pretreatment and enzymatic hydrolysis (a); lignin content in recycled residue and DES recovery rate (b).

ChCl/BDO/$AlCl_3$, as presented in Fig. 5. This ternary DES system demonstrated high efficacy for the pretreatment of wheat, rice, corncob, and corn straw, achieving lignin extraction rates exceeding 70%. Notably superior performance was achieved for the pretreatment of rice straw, with a lignin extraction rate of 87.98%, polysaccharide degradation rate of 99.81%, and reducing sugar yield of 75.01%. These values all exceeded the metrics for wheat straw. Overall, these results demonstrate broad applicability across diverse lignocellulosic feedstocks.

3.7. Recycling of DES

As an innovative and eco-friendly solvent for lignocellulosic pretreatment, the industrial application of DESs is predominantly hindered by cost considerations. Consequently, the recycling of DESs emerges as a pivotal factor in ensuring their economic feasibility, significantly influencing both the cost-effectiveness and environmental sustainability of the pretreatment process.[37] By exploring the reuse of recycled ChCl/BDO/$AlCl_3$ for wheat straw pretreatment, this study investigates the impact of DES reuse on wheat straw pretreatment and enzymatic hydrolysis. Fig. 6(a) shows that after four recycling cycles, the lignin extraction rate decreased from 81.51% in the first recycling to 68.22%, while the residue recovery rate increased from 51.25% to 55.38%. The 72-hour polysaccharide degradation rate and reducing sugar yield demonstrated slight reductions (5.17% and 7.21%, respectively), albeit maintaining relatively high levels. Fig. 6(b) reveals that the lignin content in the recovered residue escalated with the number of recycling cycles, surging from 7.94% to 12.64%. Notably, the recovery rate of DES consistently exceeded 90% across each batch, peaking at 94.72%. These findings suggest that DES retains its efficacy even after four recycling cycles, with recovery rates exceeding 90%. Although the efficiencies of pretreatment and enzymatic hydrolysis gradually diminish with successive cycles, the decline remains moderate. This phenomenon can be primarily attributed to the weakening of hydrogen bond networks between DES molecules and the heightened viscosity of the recovered liquid, which collectively impair its capacity to dissolve and separate lignin.[35]

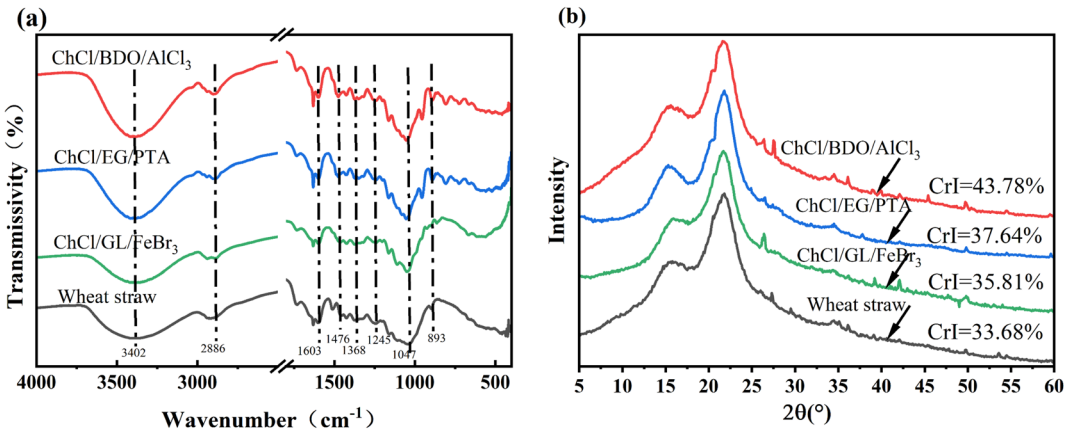

Fig. 7 FTIR (a) and XRD (b) analysis of wheat straw before and after different ternary DES pretreatments.

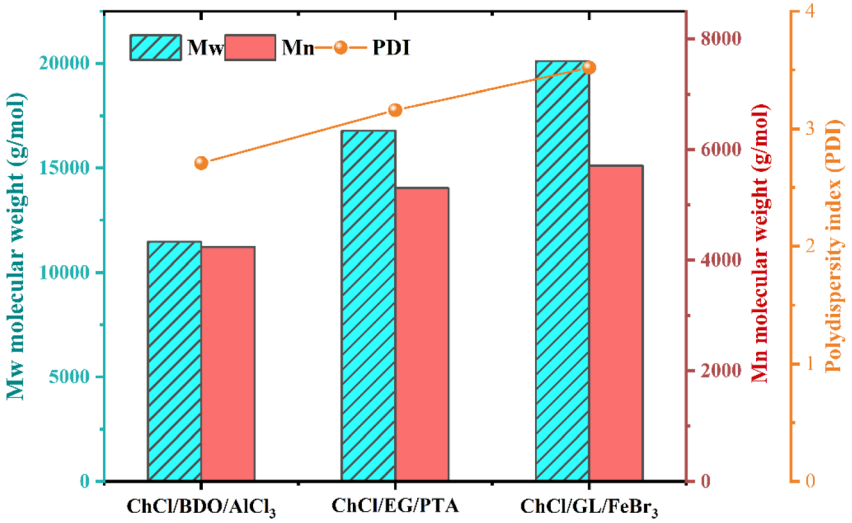

Fig. 8 The molecular weight and polydispersity index of lignin obtained by different DES pretreatments.

3.8. Characterization and analysis of raw materials and solid residues

FTIR spectra of the raw wheat straw biomass and solid residues obtained after pretreatment are shown in Fig. 7(a). Compared to the untreated wheat straw, DES pretreatment minimally altered the cellulose structure but significantly modified the lignin and hemicellulose. The FTIR spectra reveal a peak at 3402 cm^{-1}, which is associated with the stretching vibration of cellulose hydroxyl groups. This suggests that cellulose has been remained from the solid residue following pretreatment.[35] Characteristic vibrations of cellulose are noted at 2886 cm^{-1} and 1368 cm^{-1} (attributed to C–H stretching vibrations) and at 1047 cm^{-1} (corresponding to C–O–C glycosidic bond), indicating alterations in crystalline regions due to pretreatment.[13,36] Peaks observed at 1603 cm^{-1} and 1476 cm^{-1} are indicative of aromatic skeleton vibrations linked to the benzene rings in lignin,[37] implying a possible formation of cellulose derivatives. The degree of C–O–C aromatic ether bond cleavage in lignin is denoted by the peak at 1245 cm^{-1}.[38] These aromatic peaks were significantly attenuated after pretreatment, and at the same time, the signal intensity at 893 cm^{-1} (β-glycosidic C–H stretching vibrations) was enhanced, corresponding to polysaccharide enrichment.[38] This spectral evolution confirms that ternary DES pretreatment effectively delignified the wheat straw biomass. Elevated peak intensities relative to the raw biomass further demonstrate that hydrogen-bond reorganization occurred within the cellulose.[39]

XRD analysis of the wheat straw biomass samples before and after pretreatment is shown in Fig. 7(b). The crystallinity index (CrI) of the untreated biomass was 33.68%, while pretreatment with ChCl/BDO/$AlCl_3$, ChCl/EG/PTA, and ChCl/GL/$FeBr_3$ led to CrI values of 43.78%, 37.64%, and 35.81%, respectively. This improvement in crystallinity was due to the removal of amorphous lignin and hemicellulose during pretreatment. Although ternary DES pretreatment affected the diffraction peak intensities, the cellulose crystalline structures remained unaltered after pretreatment, which was consistent with the FTIR analysis. Notably, ChCl/BDO/$AlCl_3$ pretreatment led to the most significant increase in CrI, which was due to the more effective removal of amorphous components by this system leading to higher crystallinity.[40]

SEM images of the untreated and pretreated wheat straw are displayed in Fig. S1. The untreated wheat straw consisted of compact, ordered microfibril bundles with smooth and intact surfaces. After pretreatment, the fibril bundles displayed looser, porous, and partially separated structures. The wheat straw treated with ChCl/BDO/$AlCl_3$ was split into elongated bundles, with fibrils exposed in disordered arrangements. This phenomenon was potentially due to the ternary DES disrupting the lignocellulosic cross-links and partially dissolving or removing the hemicellulose and lignin. These changes increased the cellulose surface area and exposed disorderly elementary fibrils, consistent with the FTIR and XRD analyses. The SEM results confirm that pretreatment caused the wheat straw to become more fragmented, enlarged the specific surface area of the fibrils, and increased the accessibility of enzyme binding sites during hydrolysis. Consequently, the enzymatic hydrolysis yield was enhanced.[41]

3.9. Characterization and analysis of lignin

The molecular weight and polydispersity index (PDI) of lignin samples extracted using different DESs were determined *via* GPC. The weight-average molecular weight (M_w) provides insight into the contribution of high-molecular-weight components, while the number-average molecular weight (M_n) characterizes the average molecular size. The PDI, on the other hand, serves as an indicator of the breadth of the

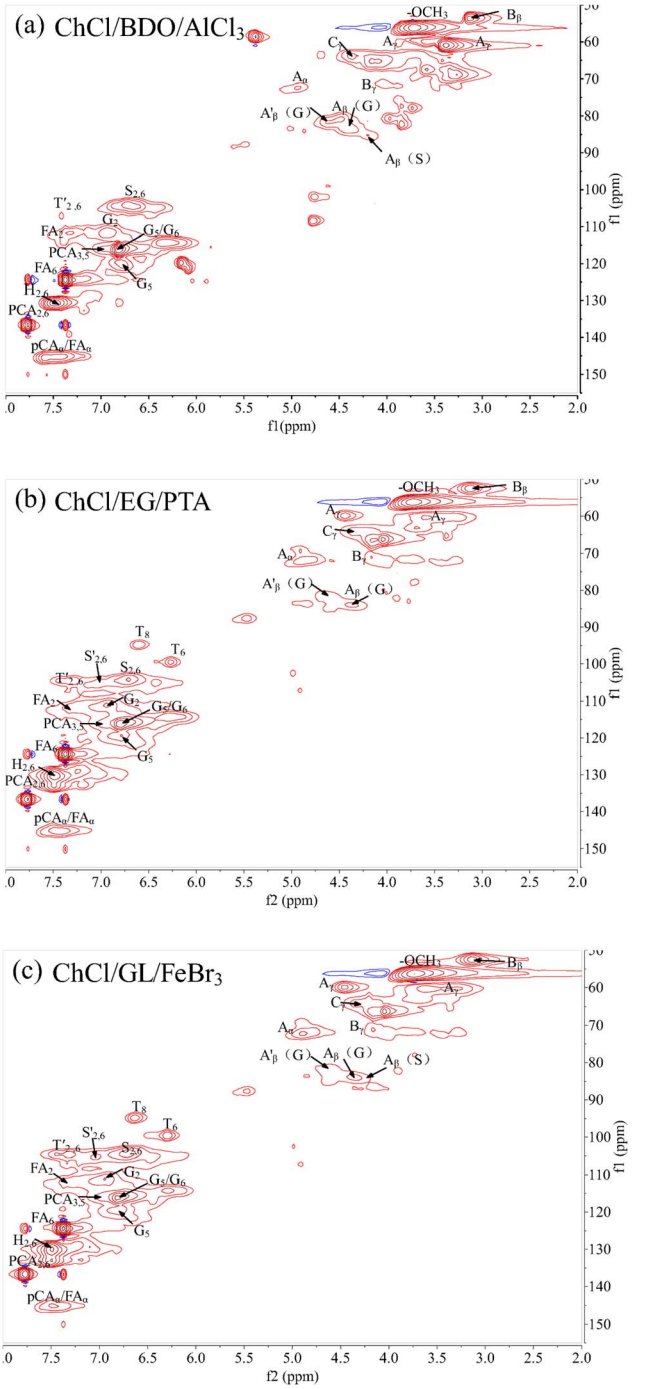

Fig. 9 2D NMR HSQC spectra of lignin: (a) ChCl/BDO/$AlCl_3$, (b) ChCl/EG/PTA, (c) ChCl/GL/$FeBr_3$.

molecular weight distribution. The results are presented in Fig. 8. The M_w and M_n values of the recovered lignin ranged from 11 465 to 20 106 g mol^{-1} and 4236 to 5709 g mol^{-1}, respectively. Among all the ternary DES pretreatments, lignin obtained through the use of ChCl/BDO/$AlCl_3$ exhibited the lowest molecular weight. This may be attributed to the potent acidity of $AlCl_3$, which effectively facilitates the cleavage of ether bonds within lignin and the lignin-carbohydrate complex (LCC).[42] In contrast, lignin derived from other DES systems displayed higher molecular weights, suggesting that the molecular size of lignin can be selectively modulated by the choice of different DES components.[13] This molecular weight characteristic is intricately linked to its subsequent application value and potential.[43]

The 2D NMR HSQC spectrum of the lignin sample in the side-chain region (δ_C/δ_H 50–90/2.0–6.0) and aromatic region (δ_C/δ_H 90–155/6.0–8.0) is displayed in Fig. 9. Based on the analysis of relevant literature,[44,45] the main characteristic peaks of lignin were assigned and are summarized in Table 3. Several intense signals are visible in the side-chain region of the NMR spectrum, such as the methoxy signal is observed at δ_C/δ_H 56.3/3.73. The C_α–H_α signal corresponding to the β-O-4′(A) linkage appears at δ_C/δ_H 72.6/4.95 ppm. Additionally, the C_β–H_β signals in the β-O-4′ structure (A) of S-type and G-type lignin units were located at δ_C/δ_H 85.2/4.20 ppm and δ_C/δ_H 83.8/4.36 ppm, respectively. In the aromatic region, signals attributable to syringyl (S), guaiacyl (G), and *p*-hydroxyphenyl (H) structures were clearly distinguishable, confirming the SGH-type structure of the analyzed lignin samples. Specifically, the 2,6-position signals in the S-type unit are detected at δ_C/δ_H 104.3/6.71 ppm. For G-type units, peak signals are observed at δ_C/δ_H 111.3/6.94 ppm (G_2), δ_C/δ_H 119.2/6.79 ppm (G_5), and δ_C/δ_H 115.9/6.79 ppm (G_6), with partial overlap noted between the G_5 and G_6 signals.

Semi-quantitative analysis was conducted using 2D HSQC NMR spectra to investigate the inter-unit linkages within lignin and their relative abundances (expressed per 100 aromatic ring units, Ar), as presented in Table 2. From the perspective of β-O-4′ bond content, the lignin obtained through ChCl/BDO/$AlCl_3$ pretreatment exhibited the lowest bond content of 5.88/100 Ar (5.88 β-O-4 ′ bonds per 100 aryl units). This value is significantly lower than that observed in lignin samples pretreated with other DES systems, indicating that the ChCl/BDO/$AlCl_3$ DES exerts the most pronounced destructive effect on β-O-4′ bonds within the lignin structure. Research has demonstrated that lignin containing a higher proportion of β-O-4′ bonds typically exhibit elevated molecular weights and more complex three-dimensional structures.[46] This finding aligns with the GPC analysis results, which revealed the lowest molecular weight for lignin pretreated with ChCl/BDO/$AlCl_3$. Regarding the *S*/*G* ratio, the *S*/*G* ratios of the lignin samples obtained from the three DES pretreatments were ChCl/BDO/$AlCl_3$ (1.23), ChCl/EG/PTA (0.42), and ChCl/GL/$FeBr_3$ (0.85). Notably, the ChCl/BDO/$AlCl_3$ pretreatment

Table 2 The semi-quantitative results of the inter-unit linkages and *S*/*G* ratio in the lignins by 2D HSQC spectra

Samples	β-O-4′	*S*/*G*
ChCl/BDO/$AlCl_3$	5.88	1.23
ChCl/EG/PTA	12.02	0.42
ChCl/GL/$FeBr_3$	17.09	0.85

Table 3 Assignment of correlation ^{13}C–^{1}H cross-signals in the 2D HSQC spectra of the lignin fractions

Lable	δ_C/δ_H (ppm)	Assignment
Side-chain–OCH3	56.3/3.73	C–H in methoxyls
A_α	72.6/4.95	C_α–H_α in β-O-4′ substructures (A)
A_γ	60.0/3.38–4.44	C_γ–H_γ in β-O-4′ substructures (A)
B_β	52.6/3.15	C_β–H_β in resinol substructures (B)
B_γ	71.2/4.17	C_γ–H_γ in resinol substructures (B)
C_γ	64.2/4.36	Cγ–Hγ in β-5′(phenylcoumaran)substructures(C)
A_β(G)	83.8/4.36	C_β–H_β in β-O-4 linked to G (A)
A_β′(G)	81.5/4.60	C_β–H_β in β-O-4 linked to G (A)
A_β(S)	85.2/4.20	C_β-H_β in β-O-4 linked to S (A,erythro)
B_α	85.5/4.63	C_α–H_α in resinol substructures(B)
Aromatic $S_{2,6}$	104.3/6.71	$C_{2,6}$–$H_{2,6}$ in syringyl units (S)
$S_{2,6}'$	105.2/7.02	$C_{2,6}$–$H_{2,6}$ in oxidized(C_αOOH)syringyl units (S)
G_2	111.3/6.94	C_2–H_2 in guaiacyl units(G)
G_5/G_6	116.4/6.83	C_5–H_5 and C_6–H_6 in guaiacyl units (G) C_5–H_5 in guaiacyl units (G)
G_5	119.2/6.79	$C_{2,6}$-$H_{2,6}$ in *p*-coumarate (*p*-CA)
$PCA_{2,6}$	136.4/7.77	$C_{3,5}$–$H_{3,5}$ in *p*-coumarate (*p*-CA)
$PCA_{3,5}$	115.3/6.86	C_α–H_α in *p*-coumarate/ferulate (*p*CA/FA)
PCA_α/FA_α	145.3/7.41	C_2–H_2 in ferulates (FA)
FA_2	111.7/7.30	C_6–H_6 in ferulates (FA)
FA_6	124.3/7.37	$C_{2,6}$-$H_{2,6}$ in *p*-hydroxyphenyl (H)
$H_{2,6}$	130.8/7.49	C_8–H_8 in tricin (T)
T_8	95.0/6.63	$C_{2,6}$–$H_{2,6}$ in tricin (T)
T_6	99.6/6.68	$C_{2,6}'$–$H_{2,6}'$ in tricin (T)
$T_{2,6}'$	104.8/7.30	

yielded the highest *S*/*G* ratio, suggesting that this treatment selectively degraded some G-type lignin units while preserving a greater proportion of S-type structures.

4 Conclusions

In this study, ternary DES systems were developed by incorporating solid acids into binary DES frameworks for wheat straw biomass pretreatment. Correlation analysis between the Kamlet–Taft solvatochromic parameters and the lignin extraction rate/enzymatic hydrolysis efficiency revealed that ternary DESs with more substantial hydrogen bond acidity exhibited superior pretreatment performance. Among these DES systems, the ChCl/BDO/$AlCl_3$ (25 : 50 : 1) system demonstrated optimal efficacy. Reaction parameter optimization was performed to determine that the best performance was achieved by pretreating the wheat straw at 120 °C for 60 min, which provided an 85.74% lignin extraction rate, 99.67% polysaccharide degradation rate, and 74.59% reducing sugar yield. Following four recycling cycles, the recovery rate of the DES consistently remained above 90%, accompanied by only marginal reductions in both pretreatment and enzymatic hydrolysis efficiency. Moreover, the optimal pretreatment conditions demonstrated broad applicability across diverse biomass types, providing an effective solution for green and efficient lignocellulose separation.

Author contributions

Jing-yuan Su: writing – original draft, visualization, investigation, formal analysis, conceptualization. Yanxia An: writing – review & editing, supervision, funding acquisition, conceptualization. Lin-lin Li: writing – review & editing, investigation, conceptualization. Jia-Zi Wang: investigation. Yi Han: investigation. Jian Zhang, supervision. Yang Zhao: supervision.

Conflicts of interest

The authors declare that they have no known competing financial interests or personal relationships that could have appeared to influence the work reported in this paper.

Data availability

Data will be made available on request.

Supplementary information is available. See DOI: **https://doi.org/10.1039/d5ra05909g**.

Acknowledgements

Financial support from the National Natural Science Foundation of China (21706052, 22278114) and Natural Science Foundation of Henan Province(242300421575)are gratefully acknowledge.The authors would like to thank all the reviewers who participated in the review and MJEditor (**https://www.mjeditor.com**) for its linguistic assistance during the preparation of this manuscript.

References

1 C. L. Yiin, K. L. Yap, A. Z. E. Ku, B. L. F. Chin, S. S. M. Lock, K. W. Cheah, A. C. M. Loy and Y. H. Chan, *Bioresour. Technol.*, 2021, **333**, 125195.
2 F. Baraka, M. M. Langari, I. Beitia, I. Dávila, J. Labidi, A. Morales and L. Sillero, *J. Environ. Chem. Eng.*, 2025, **13**, 117087.
3 A. R. Mankar, A. Pandey, A. Modak and K. K. Pant, *Bioresour. Technol.*, 2021, **334**, 125235.
4 P. Li, T. Li and S. Wu, *Int. J. Biol. Macromol.*, 2024, **280**, 136053.
5 Z. Chen, X. L. Bai, A. Lusi and C. X. Wan, *ACS Sustain. Chem. Eng.*, 2018, **6**, 12205–12216.
6 S. L. Sunar, R. K. Oruganti, D. Bhattacharyya, D. Shee and T. K. Panda, *J. Ind. Eng. Chem.*, 2024, **139**, 539–553.
7 C. Alvarez-Vasco, R. S. Ma, M. Quintero, M. Guo, S. Geleynse, K. K. Ramasamy, M. Wolcott and X. Zhang, *Green Chem.*, 2016, **18**, 5133–5141.
8 Y. T. Tan, G. C. Ngoh and A. S. M. Chua, *Ind. Crops Prod.*, 2018, **123**, 271–277.
9 J. Jiang, N. C. Carrillo-Enríquez, H. Oguzlu, X. S. Han, R. Bi, M. Y. Song, J. N. Saddler, R. C. Sun and F. Jiang, *ACS Sustain. Chem. Eng.*, 2020, **8**, 7182–7191.
10 N. Arshad, E. J. Panakkal, A. Chantarasiri, P. Pornwongthong, H. El Bari, W. Fatriasari, P. Tantayotai and M. Sriariyanun, *Bioresour. Technol. Rep.*, 2025, **31**, 102190.
11 J. Jiang, N. C. Carrillo-Enríquez, H. Oguzlu, X. Han, R. Bi, M. Song, J. N. Saddler, R.-C. Sun and F. Jiang, *ACS Sustain. Chem. Eng.*, 2020, **8**, 7182–7191.
12 Z.-K. Wang, H. Li, X.-C. Lin, L. Tang, J.-J. Chen, J.-W. Mo, R.-S. Yu and X.-J. Shen, *Bioresour. Technol.*, 2020, **307**, 123237.
13 Y. Feng, T. L. Eberhardt, F. Meng, C. Xu and H. Pan, *Bioresour. Technol.*, 2024, **400**, 130666.
14 H. Rajapakse, R. Raviadaran and D. Chandran, *Results Eng.*, 2025, **26**, 105188.
15 Y. Oh, S. Park, D. Jung, K. K. Oh and S. H. Lee, *Int. J. Biol. Macromol.*, 2020, **165**, 187–197.
16 L. Zhang, H. Yu, S. Liu, Y. Wang, T. Mu and Z. Xue, *Ind. Eng. Chem. Res.*, 2023, 11723–11734.
17 J. H. Sanders, P. Tiller, S.-M. Cho, R. Venditti and S. Park, *Int. J. Biol. Macromol.*, 2025, **320**, 146086.
18 Q. Q. Xia, Y. Z. Liu, J. Meng, W. K. Cheng, W. S. Chen, S. X. Liu, Y. X. Liu, J. Li and H. P. Yu, *Green Chem.*, 2018, **20**, 2711–2721.
19 X. D. Hou, A. L. Li, K. P. Lin, Y. Y. Wang, Z. Y. Kuang and S. L. Cao, *Bioresour. Technol.*, 2018, **249**, 261–267.
20 B. Soares, D. J. P. Tavares, J. L. Amaral, A. J. D. Silvestre, C. S. R. Freire and J. A. P. Coutinho, *ACS Sustain. Chem. Eng.*, 2017, **5**, 4056–4065.
21 Y. Wang, X. Meng, K. Jeong, S. Li, G. Leem, K. H. Kim, Y. Pu, A. J. Ragauskas and C. G. Yoo, *ACS Sustain. Chem. Eng.*, 2020, **8**, 12542–12553.

22 J.-L. Wen, T.-Q. Yuan, S.-L. Sun, F. Xu and R.-C. Sun, *Green Chem.*, 2014, **16**, 181–190.
23 C. Florindo, A. J. S. McIntosh, T. Welton, L. C. Branco and I. M. Marrucho, *Phys. Chem. Chem. Phys.*, 2018, **20**, 206–213.
24 L. D. Weng and M. Toner, *Phys. Chem. Chem. Phys.*, 2018, **20**, 22455–22462.
25 X. Liang, Y. Zhu, B. Qi, S. Li, J. Luo and Y. Wan, *Bioresour. Technol.*, 2021, **336**, 125312.
26 R. B. Tian, M. Zhang, Y. M. Zhu, K. J. Wu, Y. Y. Liu, B. S. Wang, H. F. Lu and B. Liang, *New J. Chem.*, 2023, **47**, 19608–19616.
27 Y. X. Yang, L. H. Zhao, J. L. Ren and B. H. He, *Processes*, 2022, **10**, 778.
28 X. Q. Lu, X. T. Feng, X. Z. Li and J. Zhao, *Bioresour. Technol.*, 2018, **267**, 110–116.
29 L. Yao, H. T. Yang, C. G. Yoo, C. X. Chen, X. Z. Meng, J. Dai, C. L. Yang, J. Yu, A. J. Ragauskas and X. Chen, *Green Chem.*, 2021, **23**, 333–339.
30 Z. Chen, Y. G. Wang, H. N. Cheng and H. B. Zhou, *Ind. Crops Prod.*, 2022, **187**, 115335.
31 Q. L. Liu, X. H. Zhao, D. K. Yu, H. T. Yu, Y. B. Zhang, Z. M. Xue and T. C. Mu, *Green Chem.*, 2019, **21**, 5291–5297.
32 Q. Yu, J. Liu, X. Zhuang, Z. Yuan, W. Wang, W. Qi, Q. Wang, X. Tan and X. Kong, *Bioresour. Technol.*, 2016, **199**, 265–270.
33 C. Ji, R. Weng, C. Yu, Y. Fan and J. Ouyang, *Ind. Crops Prod.*, 2025, **227**, 120779.
34 J. Cheng, C. Huang, Y. Zhan, S. Han, J. Wang, X. Meng, C. G. Yoo, G. Fang and A. J. Ragauskas, *Chem. Eng. J.*, 2022, **443**, 136395.
35 X. Chen, Q. Liu, B. Li, N. Wang, C. Liu, J. Shi and L. Liu, *Int. J. Biol. Macromol.*, 2024, **259**, 129354.
36 X. Zhao, W. Tang, B. Fan, Y.-C. He and C. Ma, *Int. J. Biol. Macromol.*, 2025, **303**, 140417.
37 V. Sharma, M.-L. Tsai, C.-W. Chen, P.-P. Sun, A. K. Patel, R. R. Singhania, P. Nargotra and C.-D. Dong, *Bioresour. Technol.*, 2022, **360**, 127631.
38 N. Kumar, P. D. Muley, D. Boldor, G. G. Coty and J. G. Lynam, *Ind. Crops Prod.*, 2019, **142**, 111865.
39 W. Liu, C. X. Ning, Z. Li, X. Y. Li, H. M. Wang and Q. X. Hou, *Ind. Crops Prod.*, 2023, **194**, 116342.
40 Y. L. Loow, T. Y. Wu, G. H. Yang, L. Y. Ang, E. K. New, L. F. Siow, J. M. Jahim, A. W. Mohammad and W. H. Teoh, *Bioresour. Technol.*, 2018, **249**, 818–825.
41 W. Wu, P. Zhu, L. Luo, H. Lin, Y. Tao, L. Ruan, L. Wang and Q. Qing, *Bioresour. Technol.*, 2024, **395**, 130338.
42 Y.-T. Yang, M.-K. Qin, Q. Sun, Y.-F. Gao, C.-Y. Ma and J.-L. Wen, *Int. J. Biol. Macromol.*, 2022, **209**, 1882–1892.
43 C. Lu, J. Xu, J. Xie, S. Zhu, B. Wang, J. Li, F. Zhang and K. Chen, *Int. J. Biol. Macromol.*, 2022, **222**, 2512–2522.
44 E. A. Capanema, M. Y. Balakshin and J. F. Kadla, *J. Agric. Food Chem.*, 2005, **53**, 9639–9649.
45 M. Y. Balakshin, E. A. Capanema, C. L. Chen and H. S. Gracz, *J. Agric. Food Chem.*, 2003, **51**, 6116–6127.
46 X.-S. Cao, X.-L. Lin, B.-Y. Li, R. C. Wu and L. Zhong, *Int. J. Biol. Macromol.*, 2024, **264**, 130475.